Seventh Cambridge Workshop on Cool Stars, Stellar Systems, and the Sun
ASP Conference Series, Vol. 26, 1992
Mark S. Giampapa and Jay A. Bookbinder (eds.)

MAGNETO-CONVECTION

ROBERT F. STEIN Michigan State University, East Lansing, MI 48824, USA

AXEL BRANDENBURG NORDITA, Blegdamsvej 17, DK-2100 Copenhagen Ø, Denmark; and Observatory and Astrophys. Lab., University of Helsinki, Tähtitorninmäki, SF-00130 Helsinki, Finland

ÅKE NORDLUND Copenhagen University Observatory, Østervoldgade 40, DK-1350, Copenhagen, Denmark

ABSTRACT Results of two simulations of magneto-convection are presented: an idealized calculation of a convective layer between two stable layers and a more realistic calculation of the upper solar convection zone applicable to a strong plage. The velocity field consists primarily of vertical vortex tubes corresponding to strong downdrafts, embedded in slow broad upflows. The magnetic field consists primarily of vertical flux tubes in the unstable layer, but is mainly horizontal in the stable layer below the convection zone. Comparison of solar magnetic and non-magnetic simulations shows that the magnetic field inhibits the magnitude of the velocity fluctuations and reduces the size of granules, in accordance with observations.

Keywords: Convection; Magneto-hydrodynamics; magnetic fields; the sun

INTRODUCTION

Convection is the mechanism of energy transport through the outer layers of all cool stars. Many such stars exhibit activity which is believed to be intimately connected with magnetic fields. We have therefore begun to explore the nature of magneto-convection using numerical simulations. Here we discuss the results of two such simulations, one idealized and the other a realistic simulation of a solar plage. The idealized simulation is of a perfect gas, in the presence of rotation, with a unstable layer sandwiched between two stable layers above and below it. The solar simulation is of the outer megameter (Mm) of the convection zone and includes radiative energy losses at the surface and an equation of state with the effects of ionization and excitation.

IDEALIZED SIMULATION

We solve the equations for conservation of mass, momentum and energy and the induction equation in a cartesian box of dimensions $63 \times 126 \times 37$ grid points. The x-axis points north, the y-axis points east and the z-axis points down. The horizontal boundaries are periodic, while the top and bottom boundaries are

impenetrable stress-free perfect conductors. A fixed incident flux is imposed at the bottom boundary and the top few layers are cooled. The equations are cast in dimensionless units with

$$d = g = \bar{\rho} = c_p = 1,$$

where d is the depth of the unstable region, time is measured in units of $(d/g)^{1/2}$ ($\approx$ the free fall time through the unstable layer), and the magnetic field in units of $(\mu_0 \bar{\rho} g d)^{1/2}$. In these units the computational domain extends 6 x 3 horizontally and from -0.15 to 1.5 vertically. The radiative conductivity is small in the unstable layer ($0 \leq z \leq 1$) and large in the stable layers ($1 \leq z \leq 1.5$). The rotation period is 43 time units, corresponding to about 30 sound crossing times. Figure 1 shows the (horizontally and temporally averaged) mean atmosphere, which extends four pressure scale heights.

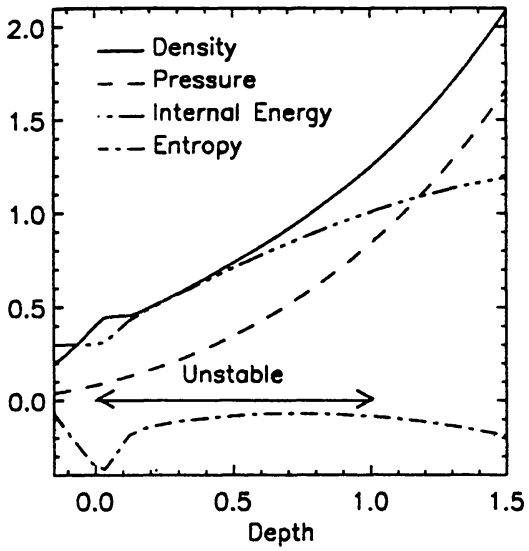

Fig. 1: Mean atmosphere of the idealized simulation.

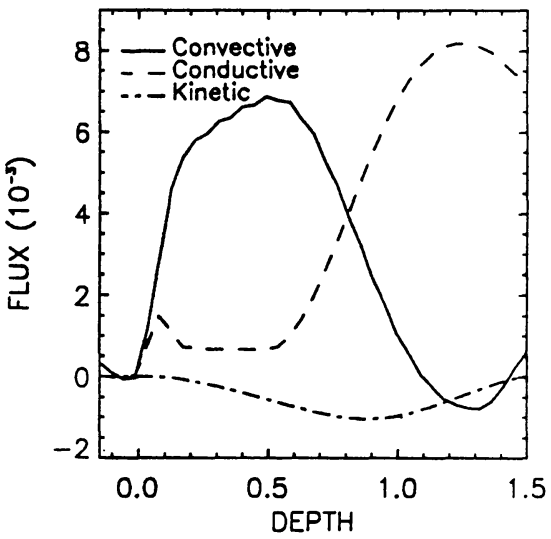

Fig. 2: Average enthalpy, kinetic energy and conductive fluxes in the atmosphere.

ENERGETICS

In the convectively unstable layer, where the thermal conductivity is small, convection carries 90% of the total flux and conduction about 10% (figure 2). There is a gradual switch over at the bottom of the convection zone and the entropy gradient becomes sub-adiabatic below the depth (0.7) where the conductive flux predominates (figure 1). Buoyancy work, which drives the motions, is positive in both the upflows and downdrafts, with most of the work being done in the downdrafts. Downdrafts as the primary site of the buoyancy work is a robust result of the various convective simulations. In the stable layer below the convection zone, the thermal conductivity is large and conduction

carries most of the energy flux. In fact, the convective flux is downward. The upflows carry no net enthalpy plus kinetic energy flux, while the downflows carry both enthalpy and kinetic energy downward. Hence, below the convection zone, the conductive flux exceeds the total flux through the atmosphere in order to compensate for the downward transport of energy by the overshooting motions. In this overshoot layer, the downflows are being braked by buoyancy (negative buoyancy work), while the upflows produce no net buoyancy work (Hurlburt *et al.* 1984). At the top of the convection zone the convective flux again goes to zero and the conductive flux starts to increase, but this increase is terminated by the removal of energy by volume cooling which is imposed in the upper 10% of the computational box. (The energy flux removed by this cooling is not shown.)

MAGNETIC FIELD

This simulation was started with a horizontal seed magnetic field which reversed its sign, so there is no net flux. Dynamo action occurs (Brandenburg *et al.* 1991). After saturation, the magnetic field in the unstable layer consists primarily of vertical flux tubes as is seen in a view of the magnetic field vectors for those locations where the field is large (figure 3). The horizontally averaged rms magnitude of the field components (figure 4) shows that the field is mainly vertical in the unstable layer and horizontal in the stable region. The magnetic energy is a maximum in the lower part of the convection zone. However, the mean magnetic field is approximately zero in the convection zone and accumulates in the stable layers above and below (figure 5). Note that the toroidal (y-) and poloidal (x-) components are approximately equal in magnitude.

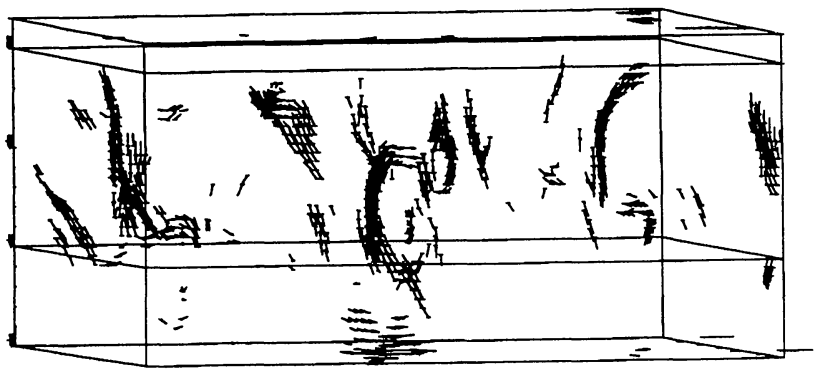

Fig. 3: Magnetic field vectors with magnitude > 43% of the maximum field strength, as seen in a 3D perspective view through the long side. The levels $z = 0$ and $z = 1$ are shown by lines around the circumference of the box.

The peakedness of the magnetic field distribution is measured by its kurtosis, $< B_i^4 > / < B_i^2 >^2$, the inverse of which is a measure of the filling

factor. A gaussian distribution would have a kurtosis of 3. Here we find the magnetic field has a kurtosis of 10, so it is much more peaked than a gaussian distribution and its filling factor is about 10%.

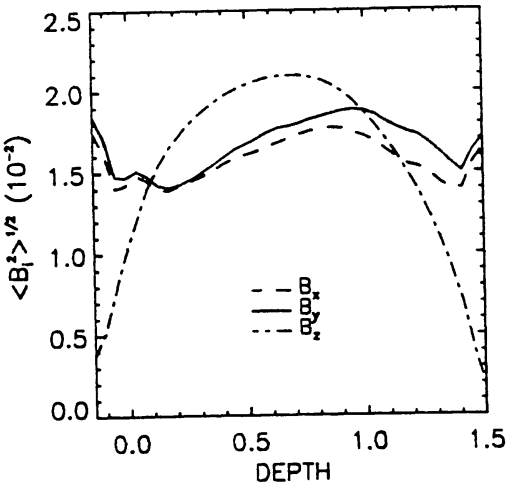

Fig. 4: Average rms magnitudes of the magnetic field components.

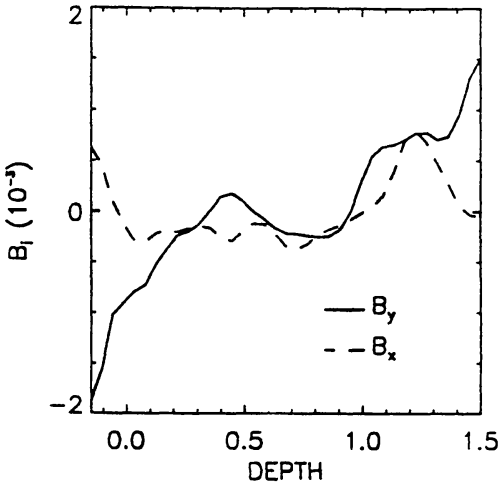

Fig. 5: Horizontal and temporal average of the magnetic field components.

VELOCITY FIELD

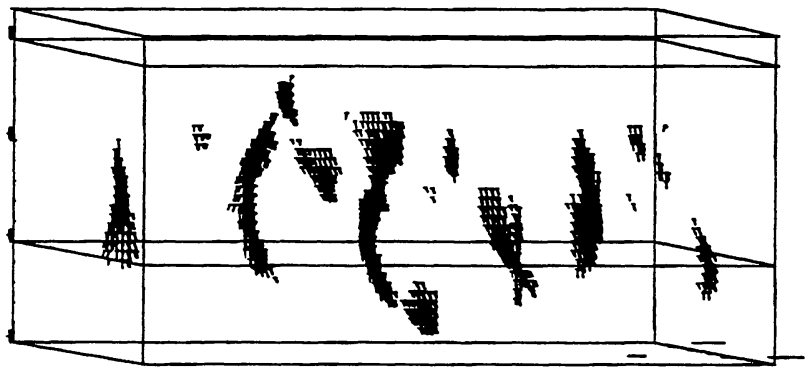

Fig. 6: Kinetic energy flux vectors for the same snapshot as fig 3. Those vectors with magnitude > 0.25% of the maximum flux are shown.

One of the most robust results of all convection simulations is that the velocity field is composed of broad regions of upflow and in the interior isolated strong downdrafts. Vectors of the kinetic energy flux (figure 6) reveal the downdrafts. Although both the velocity and magnetic field exhibit vertical structures in the convective zone, the velocity field has a much larger filling factor (its kurtosis ≈ 3, so its filling factor is about 30%).

This model has a mean rotation and it is interesting to look at its differential rotation (v_y). Figure 7 shows that the differential rotation decreases inward in the upper part of the convection zone, then increases through the bottom three quarters of the convection zone, and finally in the lower stable layer decreases again. Note also that the meridional (north-south, v_x) flow is roughly comparable to the differential rotation.

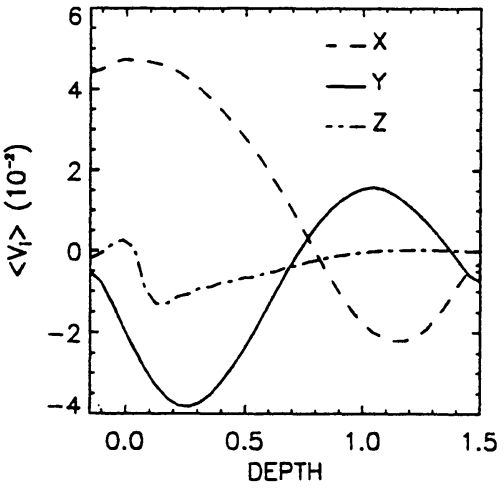

Fig. 7: Horizontally and temporally averaged velocity components. The x-component is the meridional flow, the y-component is the differential rotation and the z-component is the vertical motion.

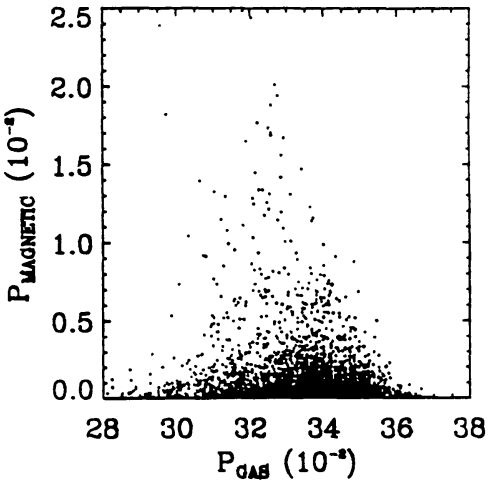

Fig. 8: Correlation of magnetic and gas pressure at $z = 0.5$.

MAGNETIC FIELD CORRELATIONS

Next we present the correlations of the magnetic field with various properties of the flow. One expects there to be a correlation between the magnetic field strength and the gas pressure and in this toy model there is, but it is weak. Where the field is strong the gas pressure is below average and where the gas pressure is above average the field is weak (figure 8). However, there is very little correlation with the density which suggests only minimal effects of magnetic buoyancy. Vorticity is organized into nearly vertical vortex tubes (figure 9), and

the magnetic field tends to be wrapped around them but avoids their cores – the field is largest where the vertical vorticity is small. From movies of the vorticity and magnetic field it is easy to see that vortices wrap the magnetic field around and push it down toward the stable layer at the bottom.

Fig. 9: Vorticity vectors scaled by $\overline{\rho}^{1/3}$ for locations where their magnitude is > 50% of the maximum value. The snapshot and viewing angle are the same as for the magnetic field vectors (fig 3) and the kinetic energy flux vectors (fig 6). (The vorticity has been scaled because the velocity decreases with depth.)

SOLAR MAGNETO-CONVECTION

The solar simulation is interesting both because it can be compared with observations of the sun and because we have run nearly the same simulation both with and without magnetic fields, so the effect of the field on the atmosphere and the convection can be seen by a differential analysis.

The magneto-convection simulation was performed on a grid 63 × 63 × 32 covering 3 × 3 × 1.5 Mm from the temperature minimum to 1 Mm below the surface. The mean vertical magnetic field is 500 gauss, which corresponds to a very strong plage region. There was no rotation in this case. The hydrodynamic simulation has the same resolution but is twice as big, covering a region 6 × 6 × 3 Mm from the temperature minimum to 2.5 Mm below the surface using a grid of 125 × 125 × 82. These calculations were not started from the identical conditions, but from similar, and statistically equivalent, convective states. The magneto-convection simulation was begun by imposing a uniform vertical field of 500 gauss on a snapshot of non-magnetic convection. Convective motions quickly swept the field to the granulation boundaries. Thereafter it slowly evolved as the granulation pattern changed (Nordlund and Stein 1990). Further discussion of the hydrodynamic convection case can be found in Stein and Nordlund (1989, 1991). We now compare these two cases.

First, consider the mean atmosphere. The temperature and entropy structure is shown in figure 10. One can see that the adiabat is about the same. In both calculations we fed in the same entropy fluid from below. The temperature is slightly higher and the region of steep temperature gradient lies slightly higher up in the atmosphere in the magneto-convection case.

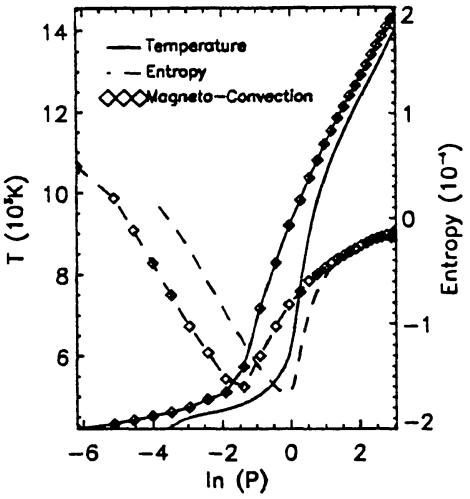

Fig. 10: Average temperature and entropy structure of the solar magneto- and hydrodynamic- convection simulations.

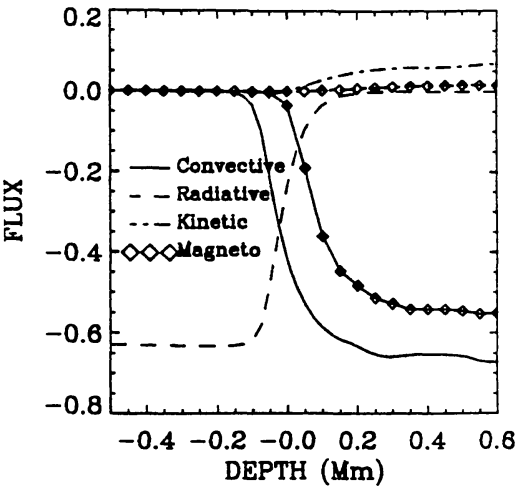

Fig. 11: Average enthalpy, radiative and kinetic energy fluxes for the solar magneto- and hydrodynamic- convection simulations.

ENERGETICS

Next consider the changes in the energetics. The magnetic field reduces the convective flux a little (figure 11). Both the enthalpy and the kinetic energy fluxes are noticeably smaller, and their sum (the net flux) is slightly reduced. This is due to a reduction in the velocity fluctuations in the magnetic case by about a factor of two in both the upward and downward flows (figure 12).

Most of the flux in this case is carried by the downflows. The upflows (negative velocities) carry the same flux in both the magnetic and non-magnetic cases. The flux carried by the downflows is however slightly smaller in the magnetic case. Which portion of the fluid, upflows or downdrafts, carries the net flux is **not** a robust result of convective simulations. It depends upon the amount of diffusion in the numerical scheme, the equation of state used and the vigor of the convection. These realistic calculations have the downdrafts carrying 70% of the flux. We have also used our code to simulate convection of an ideal gas in a rigid box with strong thermal conduction as described in Cattaneo *et al.* (1991). In that case, we too found cancellation of the enthalpy and kinetic energy fluxes in the downdrafts, with most (70%) of the net flux

carried in the upflows (just the reverse of our realistic simulations). The extent of cancellation is not as complete in our case as in Cattaneo *et al.* because our code was more diffusive. The inescapable conclusion is that where the flux in a simulation is transported depends on the physics included in the calculation.

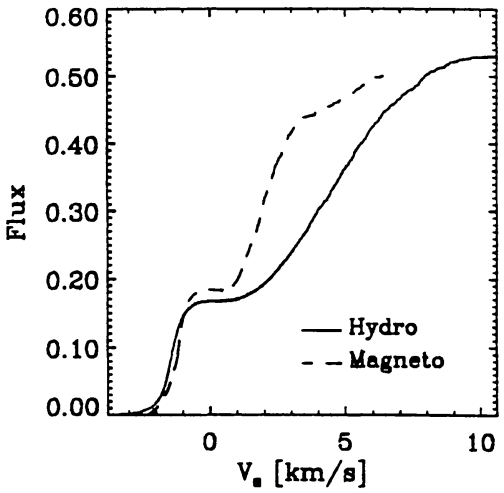

Fig. 12: Sum of the net flux $F_{net} = F_{enthalpy} + F_{kinetic\ energy}$ contributions as a function of velocity fluctuation at $z = 0.5$ Mm. Downflows are positive velocity and upflows negative.

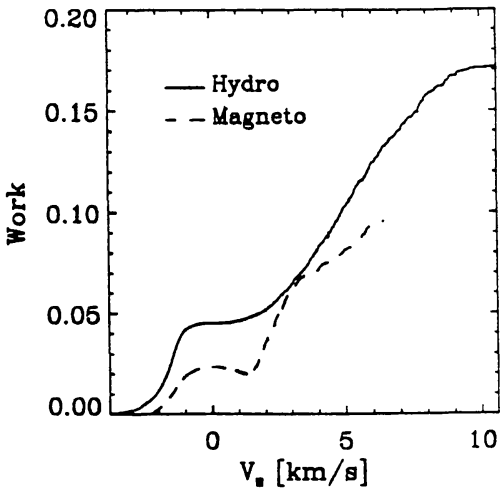

Fig. 13: Sum of the buoyancy work contributions as a function of velocity fluctuation at $z = 0.5$ Mm.

The major difference between the magnetic and non-magnetic cases is in the buoyancy work. The magnetic field significantly reduces the buoyancy work in both the upflows and downflows (figure 13).

MAGNETIC FIELD

The magnetic field is concentrated into the downflows by the horizontal velocity field. The horizontal motions of the granules sweep the field out of the granules into the intergranule lanes. Below the surface there is a significant difference in the flow topology. In the non-magnetic case the connected downflows break up into isolated downdrafts within a short distance below the surface. In the magnetic case, with its strong (500 gauss average) field, the magnetic field tends to act as rigid walls to the granule flow and make the connected downflows extend much deeper than they do in the field free case.

Again, we can look at the correlations of the magnetic field and gas properties. There is a very tight anti-correlation between the magnetic and gas pressure. Where the magnetic field is strong the gas pressure is low and vice versa (figure 14). This is much tighter than in the idealized simulation, because the magnetic pressure is closer in magnitude to the gas pressure here.

An anti-correlation with the density also occurs, because that is the primary means for reducing the pressure. The magnetic field is swept by the diverging upflows toward the downflows where it accumulates and impedes the horizontal flow (across field lines). This reduced inflow quenches the downflow as well. As a consequence, magnetic fields tend to correlate with low temperatures, low densities and small downward velocities.

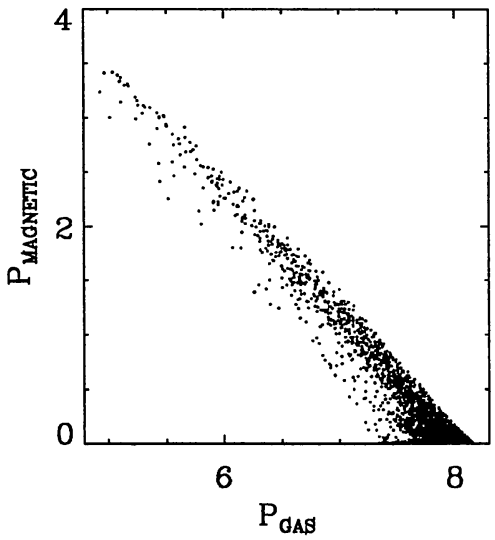

Fig. 14: Magnetic and gas pressure correlation for the solar simulations at a depth of 0.5 Mm.

OBSERVABLE EFFECTS

A magnetic field has a readily observable effect on the size of the granulation. Figure 15 shows a comparison of the emergent intensity in the magnetic and non-magnetic cases. The granules are smaller in the presence of magnetic field as described by Title (1992). This together with the inhibition of velocity fluctuations by the magnetic field are two easily observable effects of magnetic fields on convection as determined by a comparison of our two simulations.

ACKNOWLEDGEMENTS

This work was supported in part by grants from the National Aeronautics and Space Administration (NAGW 1695), the Danish Natural Science Research Council and the Danish Space Board. The simulations were performed on the Alliant FX-8 at the University of Colorado, the Cray-2 at the National Center for Supercomputer Applications, the Convex 240 at MSU, and the Cray X-MP/432 of the Centre for Scientific Computing in Finland. The authors wish to express their appreciation for the support from these agencies. We also thank Juha Ruokolainen for help in preparing videos of the simulations.

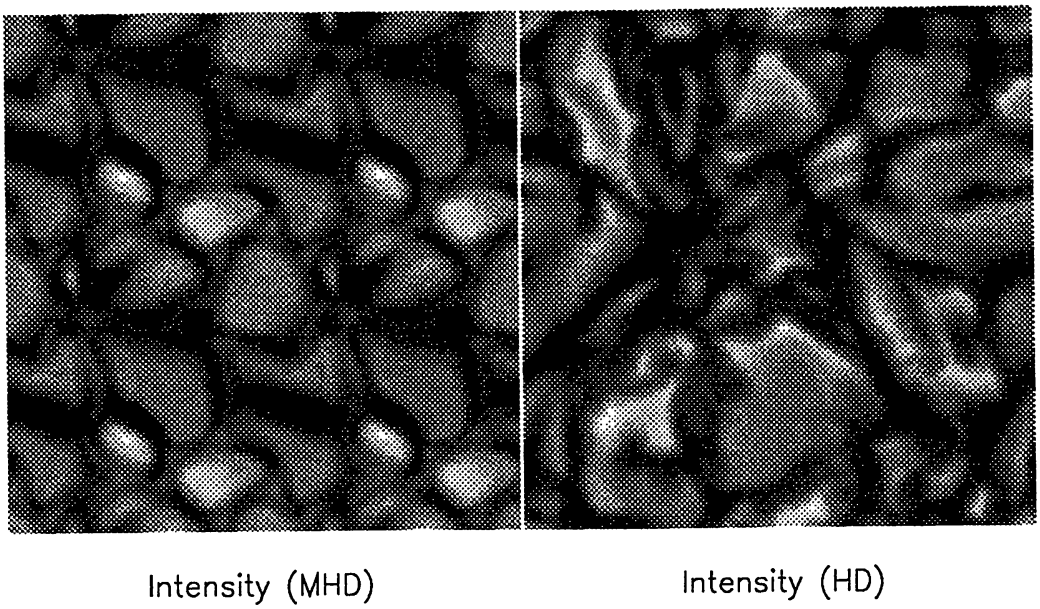

Fig. 15: Comparison of emergent intensity patterns (granulation) for the solar magneto- and hydrodynamic- convection simulations.

REFERENCES

Brandenburg, A., Jennings, R. L., Nordlund, Å., Stein, R. F. and Tuominen, I. 1991. "The role of overshoot in solar activity: A direct simulation of the dynamo," in The Sun and Cool Stars: Activity, Magnetism, Dynamos, IAU Coll. 130, eds. I. Tuominen, D. Moss & G. Rüdiger, Lecture Notes in Physics, Springer-Verlag, p. 86.

Cattaneo, F., Brummell, N.H., Toomre, J., Malagoli, A. and Hurlburt, N.E. 1991. "Turbulent Compressible Convection", *Ap. J.*, **370**, 282.

Hurlburt, N.E., Toomre, J. and Massaguer, J.M. 1984. "Two-Dimensional Compressible Convection Extending Over Multiple Scale Heights", *Ap. J.*, **282**, 557.

Nordlund, Å. and Stein, R. F. 1990. "Solar Magnetoconvection", in Solar Photosphere: Structure, Convection, Magnetic Fields, IAU Symp. 138, ed. J. O. Stenflo, p. 191.

Stein, R. F. and Nordlund, Å. 1989. "Topology of Convection Beneath the Solar Surface", *Ap. J. Letters*, **342**, L95.

Stein, R. F. and Nordlund, Å. 1991. "Convection and its Influence on Oscillations", in Challenges to Theories of the Structure of Moderate Mass Stars, eds. J. Toomre and D. Gough, Lecture Notes in Physics **388**, (Springer-Verlag: Berlin), p. 195.

Title, A. 1992 this conference.